



# Effect of strain hardening on texture development in cold rolled Al–Mg alloy

W.C. Liu<sup>a,\*</sup>, C.-S. Man<sup>b</sup>, D. Raabe<sup>c</sup>

<sup>a</sup> Key Laboratory of Metastable Materials Science and Technology, College of Materials Science and Engineering, Yanshan University, Qinhuangdao 066004, China

<sup>b</sup> Department of Mathematics, University of Kentucky, 715 Patterson Office Tower, Lexington, KY 40506, USA

<sup>c</sup> Max-Planck-Institut für Eisenforschung, Microstructure Physics, Max-Planck-Str. 1, 40237 Düsseldorf, Germany

## ARTICLE INFO

### Article history:

Received 19 August 2009

Received in revised form

26 September 2009

Accepted 29 September 2009

### Keywords:

Aluminum

Cold rolling

Texture

X-ray diffraction

Strain hardening

## ABSTRACT

The hot band of a continuous cast Al–Mg alloy possesses a typical deformed structure and a strong  $\beta$  fiber rolling texture. The hot band was heat-treated at 260 °C for 3 h to generate different degrees of strain hardening. The hot band and its counterpart after recovery treatment were cold rolled to different reductions along the original transverse direction. The effect of strain hardening on texture evolution was investigated by X-ray diffraction. The results show that a high degree of strain hardening reduces the formation rate of the  $\beta$  fiber rolling texture.

© 2009 Elsevier B.V. All rights reserved.

## 1. Introduction

The evolution of crystallographic texture during the rolling of aluminum alloys has long been a subject of research as the anisotropy of mechanical properties is significantly influenced by the texture developed during processing. During rolling initial orientations are gradually rotated into more stable texture components located on the  $\beta$  fiber component, which runs from the brass (B) orientation  $\{110\}\langle 112 \rangle$  through the S orientation  $\{123\}\langle 634 \rangle$  to the copper (C) orientation  $\{112\}\langle 111 \rangle$  [1–4]. Texture evolution during rolling is strongly affected by alloy composition, initial microstructure and texture prior to cold rolling. It is widely established that the initial texture has a large impact on rolling texture evolution [5–9]. The formation rate of the  $\beta$  fiber decreases as the initial texture changes from the *r*-cube texture to the cube texture [9]. The strong impact of the initial texture on rolling texture may overshadow the influence of other material parameters. It has been shown that a decrease in initial grain size leads to an accelerated rate of rolling texture evolution [10–12].

The development of rolling textures is related to the dislocation structures introduced during rolling. During plastic deformation initial grains are subdivided into dislocation cells due to the formation of dislocation boundaries [13–15]. The spacing between dislocation boundaries decreases with increasing strain, while the

misorientation angle across dislocation boundaries increases. This results in an increase in the stored energy of deformation and the strain hardening of the material. In the classical Taylor model, the texture predictions are independent of strain hardening and grain size. In advanced texture models such as the grain interaction (GIA) [16–19] and crystal plasticity finite element models [20–24], however, the influence of grain interaction, yield strength, strain hardening, and grain size on texture evolution is taken into consideration. The objective of the research reported here is to examine the influence of different degrees of strain hardening on rolling texture through experimental work. In order to carry out this work, it is of key importance to study samples of the material that have different degrees of strain hardening while holding the other parameters fixed.

The hot band of continuous cast (CC) aluminum alloys possesses a typical deformed structure and a strong  $\beta$  fiber rolling texture. Recovery treatment of the hot band decreases the degree of strain hardening due to changes in the dislocation structure of the material, but does not alter the  $\beta$  fiber rolling texture. Further rolling of the hot band along the original rolling direction will incrementally strengthen the  $\beta$  fiber rolling texture. But it will be difficult to determine the effect of strain hardening on texture evolution from such incremental changes. Under cross-rolling (i.e., along the original transverse direction (TD)), on the other hand, the former  $\beta$  fiber orientations are unstable and they will gradually rotate towards the  $\beta$  fiber in the new sample reference system [25]. The resulting huge changes in rolling textures will allow accurate determination of the effect of strain hardening on texture evolution.

\* Corresponding author. Tel.: +86 15833356275; fax: +86 335 8074545.

E-mail address: [wcliu@ysu.edu.cn](mailto:wcliu@ysu.edu.cn) (W.C. Liu).

## 2. Experimental

The material used in the present investigation was AA 5005 aluminum alloy. The chemical composition of this alloy is given in Table 1. The as-received material was a CC hot band, which was produced using standard industrial practices. The thickness of the hot band of the CC AA 5005 aluminum alloy was 2.54 mm. The hot band was heat-treated at 260 °C for 3 h in an air furnace to

**Table 1**

Chemical compositions of CC AA 5005 aluminum alloy (wt%).

Alloy	Si	Fe	Cu	Mn	Mg	Cr	Al
5005	0.147	0.431	0.013	0.121	0.962	0.042	Bal

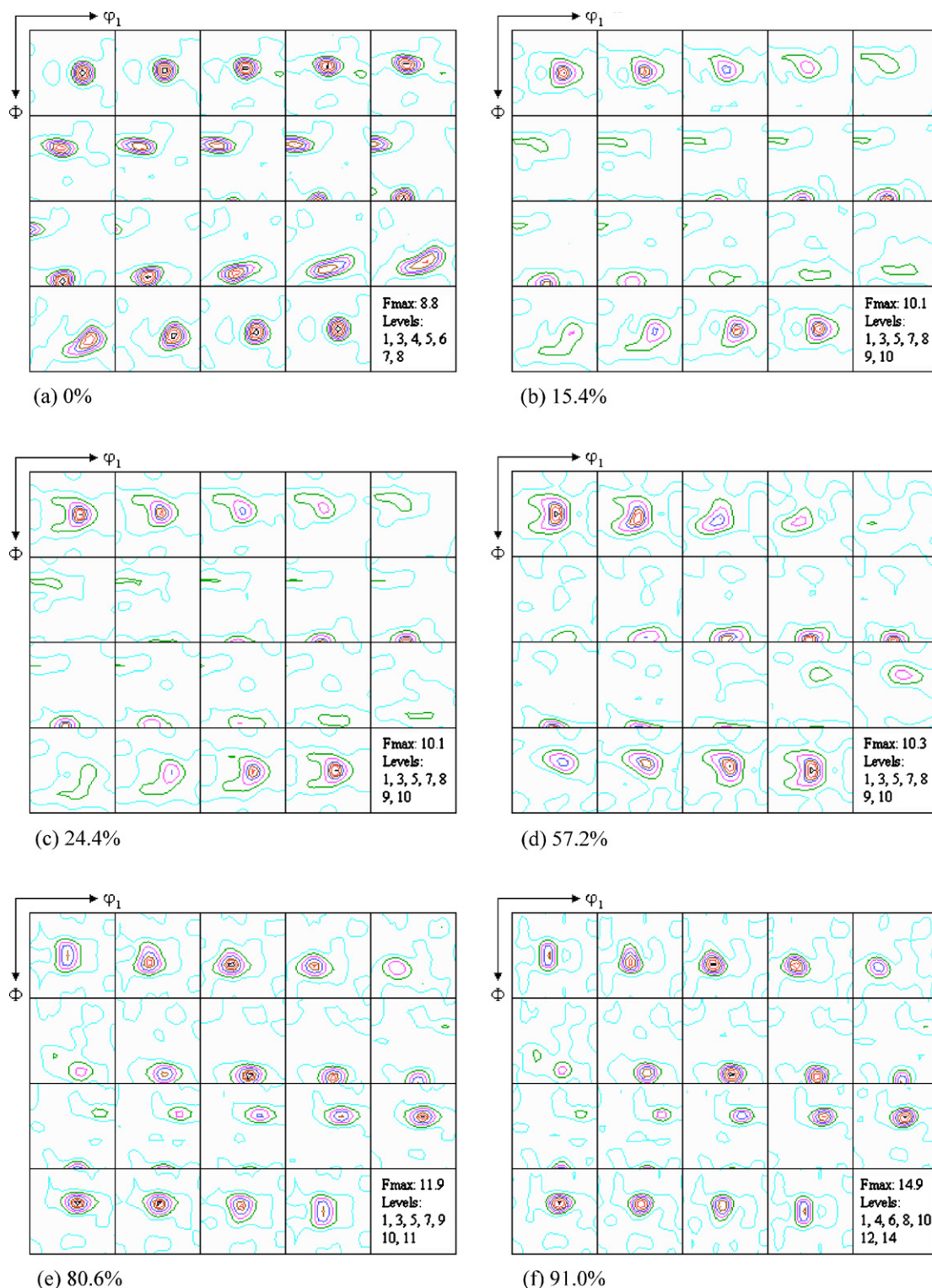


**Fig. 1.** Texture evolution of CC AA 5005 hot band during cold rolling along the original TD.

generate different degrees of strain hardening through recovery of the deformed microstructure. The yield strength, ultimate tensile strength and elongation of the hot band were measured to be 204, 229 MPa and 11.9%, respectively. After the recovery treatment, the yield strength and ultimate tensile strength decreased to 174 and 196 MPa, respectively, while the elongation slightly increased to 12.3%. Both the hot bands in the as-rolled state and in its state after the recovery treatment were then cold rolled to different reductions ranging from 0% to 91% along the original transverse direction (TD) on a laboratory rolling mill with rolls of 103 mm in diameter.

Texture measurements were performed at the quarter thickness of the cold rolled sheets. The (1 1 1), (2 0 0), and (2 2 0) pole figures were measured up to a maximum tilt angle of  $75^\circ$  by the Schulz back-reflection method using Cu  $K\alpha$  radiation. The orientation distribution functions (ODFs) were calculated from the incomplete pole figures using the series expansion method ( $l_{\max} = 16$ ) [26]. The ODFs were presented as plots of constant  $\varphi_2$  sections with isointensity contours in Euler space defined by the Euler angles  $\varphi_1$ ,  $\Phi$ , and  $\varphi_2$ . The volume fractions of the texture components were calculated by an improved integration method [27,28].

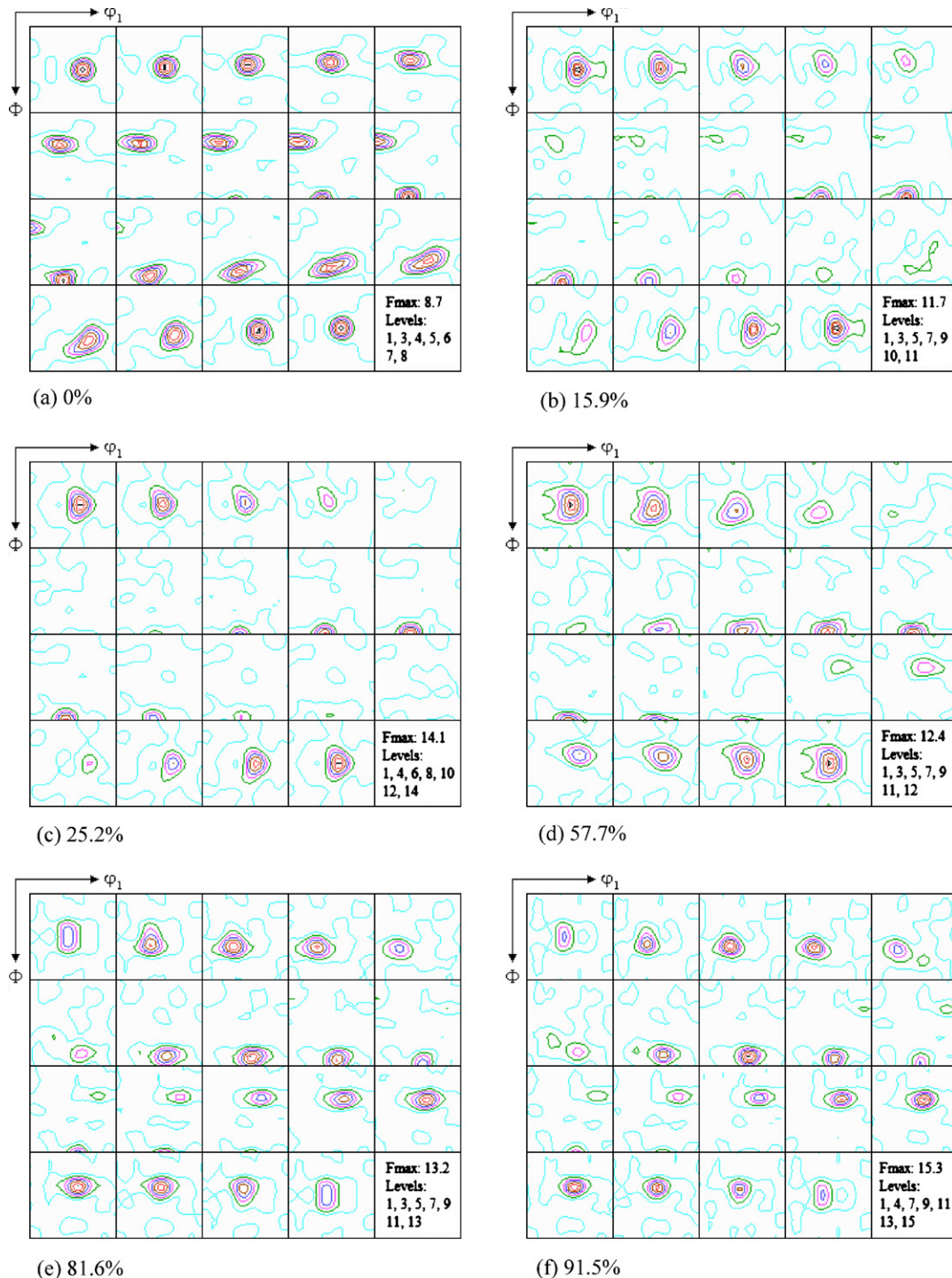


Fig. 2. Texture evolution of CC AA 5005 hot band after recovery treatment during cold rolling along the original TD.



### 3. Results

The texture evolution of the as-received CC AA 5005 hot band and that of its recovery-treated counterpart during cold rolling along the original TD are shown in Figs. 1 and 2, respectively. The as-received hot band possessed a strong  $\beta$  fiber rolling texture. The recovery treatment did not alter the strength of the  $\beta$  fiber rolling texture. After  $90^\circ$  rotation about the ND, the orientations of the former  $\beta$  fiber became unstable in the new sample coordinate system as defined by the new rolling direction. During rolling all the initial orientations were gradually rotated to the  $\beta$  fiber in the current sample frame. After 91% rolling reduction, a strong  $\beta$  fiber rolling texture was observed.

A very condensed and comprehensive method for presenting the  $\beta$  fiber rolling texture is given in Fig. 3, where the intensities of orientations along the centerline of the  $\beta$  fiber are plotted as a function of the angle  $\varphi_2$ . It is noted that the intensities of the B and S orientations increased markedly with increasing rolling reduction, but the intensity of the C orientation increased slightly after about 70% rolling reduction. At large reductions, the maximum intensity of the  $\beta$  fiber was located at  $\varphi_2 = 70^\circ$ , which became a dominant rolling texture component. This suggests that the orientations of the former  $\beta$  fiber are mainly rotated into the  $\beta$  fiber between the B and S orientations during cross-rolling, leading to a faster increase in the intensities of the B and S orientations than the C orientation. The different degrees of strain hardening generated by recovery treatment prior to cold rolling had no significant effect on the distribution of orientation intensities along the  $\beta$  fiber.

The texture evolution during rolling can be analyzed quantitatively in terms of the variation in certain texture component volume fractions with rolling reduction. The volume fractions of the cube,  $r$ -cube  $\{001\}\{110\}$ , Goss  $\{011\}\{100\}$ ,  $r$ -Goss  $\{011\}\{011\}$ ,

$\beta$  fiber and remainder components, which were calculated by an improved integration method [27,28], are plotted in Fig. 4 as a function of true rolling strain. With increasing strain the volume fractions of the  $r$ -Goss and the remainder components decreased, whereas the volume fraction of the  $\beta$  fiber increased. The volume fraction of the Goss component first increased with increasing true rolling strain. When the true rolling strain reached the range of 1.2–2.4, the volume fraction of the Goss component changed slightly. The volume fractions of the cube and  $r$ -cube components were very small in the initial materials and varied slightly with strain.

In order to quantify the texture evolution during rolling, we have established an empirical relationship between the texture volume fractions and the true rolling strain [27,28]. In general, the variation in the texture volume fractions with the true rolling strain is defined by

$$f_i = \frac{M_i - M_{i0}}{M_{i\infty} - M_{i0}} \quad (1)$$

where  $M_{i0}$ ,  $M_i$  and  $M_{i\infty}$  are the texture volume fractions prior to deformation, at true rolling strain  $\varepsilon$  and at the end of the texture forming process, respectively. For the remainder component, the  $M_{i\infty}$  value is 0, while the  $M_{i\infty}$  value is 1 for the  $\beta$  fiber component. The relationship between  $f_i$  and true strain  $\varepsilon$  is formulated in the form of a Johnson–Mehl–Avrami–Kolmogorov (JMAK) equation:

$$f_i = 1 - \exp(-k_i \varepsilon^{n_i}) \quad (2)$$

where  $k_i$  is an empirical constant, and  $n_i$  is the strain exponent for the  $\beta$  fiber and the remainder component. The data for the  $f_i$  can be presented in the form of a  $\ln[-\ln(1 - f_i)]$  vs.  $\ln \varepsilon$ , as shown in Fig. 5. The values of  $k_i$  and  $n_i$  were determined by fitting the experimental data using Eq. (2). Table 2 shows the values of  $k_i$  and  $n_i$  as well as

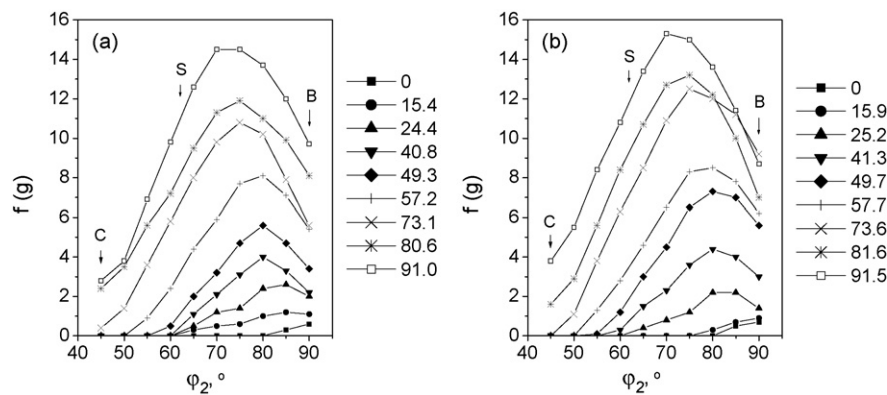


Fig. 3. Intensities of the ODF  $f(g)$  at the centerline of the  $\beta$  fiber as a function of a particular angle  $\varphi_2$  in cold rolled CC AA 5005 aluminum alloy (a) without and (b) with recovery treatment.

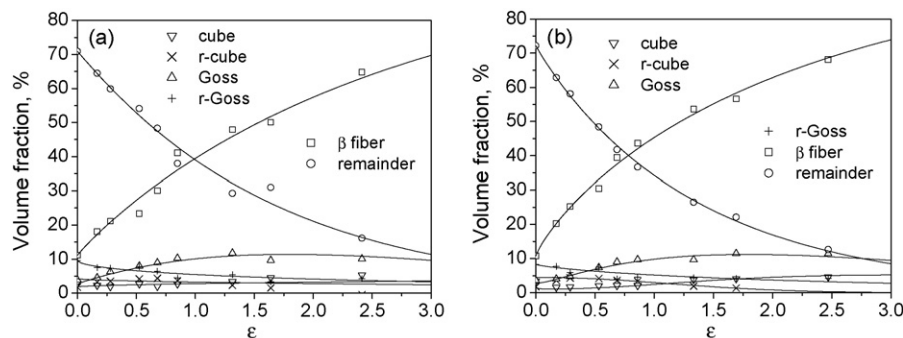


Fig. 4. Plots of texture volume fractions as a function of true rolling strain for CC AA 5005 hot band (a) without and (b) with recovery treatment. Points with different symbols are measured values, and sold lines are simulated results.

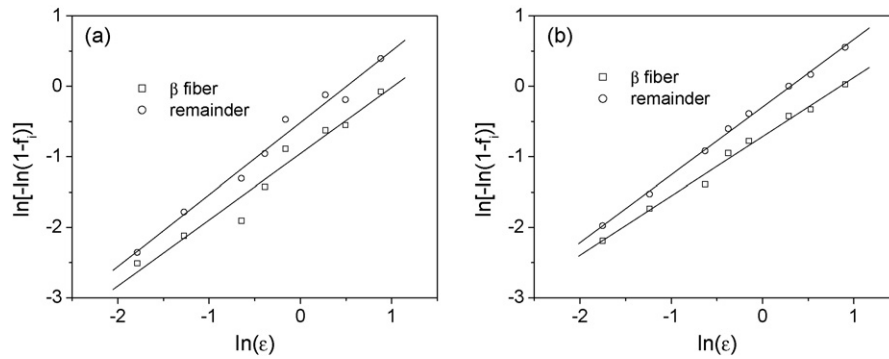


Fig. 5.  $\ln[-\ln(1-f_i)]$  vs.  $\ln \varepsilon$  for CC AA 5005 hot band (a) without and (b) with recovery treatment.

Table 2

Values of  $k_i$  and  $n_i$  in Eq. (2) for CC AA 5005 aluminum alloy.

Recovery treatment	Texture component	$M_{10}$ (%)	$k_i$	$n_i$	$r$
No	$\beta$ fiber	11.1	0.38 (0.36–0.41)	$0.94 \pm 0.08$	0.980
	Remainder	70.9	0.60 (0.57–0.63)	$1.02 \pm 0.06$	0.991
260 °C, 3 h	$\beta$ fiber	10.8	0.49 (0.47–0.50)	$0.84 \pm 0.03$	0.995
	Remainder	72.2	0.74 (0.73–0.76)	$0.96 \pm 0.02$	0.999

the correlation coefficients ( $r$ ) of these linear fits. The parameters  $M_{10}$ ,  $k_i$  and  $n_i$  describe the formation or disappearance of a given texture component during rolling. We use this fitting procedure to extract the dependence of the evolution of the texture components on material parameters. This allows more accurate determination of the effect of strain hardening on rolling texture evolution than direct comparison of the raw experimental data.

#### 4. Discussion

The texture of the CC hot band consists mainly of the  $\beta$  fiber, which runs from the B orientation through the S orientation to the C orientation. After 90° rotation about the ND, the B, S and C orientations are transformed into the  $B'$  {1 1 0}<1 1 1>,  $S'$  {1 2 3}<1 7 2 9> and  $C'$  {1 1 2}<1 1 0> orientations. These orientations were unstable in the new sample coordinate system. During cold rolling the initial orientations were gradually rotated into the  $\beta$  fiber in the new sample reference frame [25]. The texture evolution during rolling can be fitted and quantified in terms of a simple relation between the main orientation components and the true rolling strain. The  $k_i$  value in Eq. (2) reflects the rate of formation or disappearance of each texture component. It is noted from Table 2 that the hot band with the recovery treatment has a higher rate of disappearance of the remainder component and a higher rate of formation of the  $\beta$  fiber component than the hot band without the recovery treatment. Since the recovery treatment does not alter the initial texture of the hot band, the differences in rolling texture evolution can be attributed to different initial microstructures in the material and different degrees of strain hardening prior to cold rolling. Thus, it is concluded that the change in dislocation structure and the decrease in the degree of strain hardening due to recovery enhance the formation of the  $\beta$  fiber rolling texture. In other words, high stored energy of deformation and high degree of strain hardening in the material retard the lattice rotation from the initial orientations to the  $\beta$  fiber during rolling and thus reduce the formation rate of the  $\beta$  fiber rolling texture.

Based on the fact that the texture evolution during rolling is affected by initial dislocation structure and degree of strain hardening, it can be inferred that the dislocations and interfaces introduced during plastic deformation, i.e. strain hardening, also has a particular effect on rolling texture. Engler et al. [16] stud-

ied texture evolution during cold rolling of aluminum alloys by using the grain interaction (GIA) model, an advanced texture model that takes interaction between next-neighbor grains into account. In the GIA model the effect of material parameters (strength and grain size) is considered for better simulation of the rolling textures of aluminum alloys. According to their work, under conditions where strain hardening is ignored, the intensity of the cube orientation in the simulated textures is considerably weaker, while the intensities along the  $\beta$  fiber rolling texture are much sharper than their counterparts in the experimental ones. This implies that the simulated textures evolve too quickly. Under conditions where the evolution of strength and of grain size induced by rolling strain are considered, however, the simulated textures are closer to the experimental textures. This suggests that the dislocations and interfaces introduced during rolling, i.e. strain hardening, retard the texture evolution during rolling. It is clear that the present experimental findings are in agreement with the simulation results. Moreover, our experimental results indirectly substantiate that the consideration of strain hardening and grain size in the GIA model is of particular importance for accurate simulation of rolling textures.

The concept that high stored energy of deformation and high degree of strain hardening retard the development of rolling texture can be applied to explain the effect of deformation temperature and strain rate on texture evolution. It has been found that material deformed at elevated temperatures exhibits a stronger rolling texture than that deformed at room temperature [29–31]. The  $\beta$  fiber rolling texture sharpens with increasing deformation temperature and decreasing strain rate [32,33]. This stronger  $\beta$  fiber rolling texture can be attributed to a decreased stored energy of deformation due to high deformation temperatures and low strain rates.

#### 5. Conclusions

The effect of strain hardening on the texture development in cold rolled CC AA 5005 aluminum alloy was investigated by X-ray diffraction. The following conclusions are drawn from this study.

- (1) The CC AA 5005 hot band possesses a typical deformed structure and a strong  $\beta$  fiber rolling texture. The recovery treatment at 260 °C for 3 h decreases the yield strength of the hot band from 204 to 174 MPa, but does not alter the  $\beta$  fiber rolling texture.

- (2) The texture evolution of the CC AA 5005 hot band and its counterpart after recovery treatment during cross-rolling was quantified by mathematical formulae of texture volume fractions and true rolling strain. This allows more accurate determination of the effect of strain hardening on rolling texture evolution than direct comparison of the raw experimental data.
- (3) The hot band without the recovery treatment has a lower rate of formation of the  $\beta$  fiber component than the hot band with the recovery treatment. This indicates that high degree of strain hardening retards the lattice rotation from the initial orientations to the  $\beta$  fiber during rolling and thus reduces the formation rate of the  $\beta$  fiber rolling texture. The strain hardening does not affect the distribution of orientation intensities along the  $\beta$  fiber.

### Acknowledgment

This work was supported by the National Natural Science Foundation of China (Grant No. 50874097).

### References

- [1] J. Hirsch, K. Lücke, *Acta Metall. Mater.* 36 (1988) 2863–2882.
- [2] O. Engler, J. Hirsch, K. Lücke, *Acta Metall. Mater.* 37 (1989) 2743–2753.
- [3] P.A. Hollinshead, T. Sheppard, *Metall. Trans. A* 20A (1989) 1495–1507.
- [4] O. Daaland, E. Nes, *Acta Mater.* 44 (1996) 1413–1435.
- [5] J. Hirsch, W. Mao, K. Lücke, *Aluminum Technology' 86: Proceedings of the International Conference, The Institute of Metals, London, 1986*, pp. 303–309.
- [6] J. Hirsch, E. Nes, K. Lücke, *Acta Metall.* 35 (1987) 427–438.
- [7] W.B. Hutchinson, A. Oscarsson, A. Karlsson, *Mater. Sci. Technol.* 5 (1989) 1118–1127.
- [8] A. Oscarsson, W.B. Hutchinson, H.E. Ekstrom, *Mater. Sci. Technol.* 7 (1991) 554–564.
- [9] W.C. Liu, T. Zhai, C.-S. Man, B. Radhakrishnan, J.G. Morris, *Philos. Mag.* 84 (2004) 3305–3321.
- [10] N. Hansen, D. Juul Jensen, *Metall. Trans. A* 17A (1986) 253–259.
- [11] M. Sindel, G.D. Köhlhoff, K. Lücke, B.J. Duggan, *Textures Microstruct.* 12 (1990) 37–46.
- [12] O. Engler, *Textures Microstruct.* 23 (1995) 61–86.
- [13] Q. Liu, D. Juul Jensen, N. Hansen, *Acta Mater.* 46 (1998) 5819–5838.
- [14] D.A. Hughes, N. Hansen, *Acta Mater.* 48 (2000) 2985–3004.
- [15] N. Hansen, X. Huang, D.A. Hughes, *Mater. Sci. Eng. A* 317 (2001) 3–11.
- [16] O. Engler, M. Crumbach, S. Li, *Acta Mater.* 53 (2005) 2241–2257.
- [17] O. Engler, *Adv. Eng. Mater.* 4 (2002) 181–186.
- [18] O. Engler, *Modell. Simul. Mater. Sci. Eng.* 11 (2003) 863–882.
- [19] D. Raabe, *Acta Metall.* 43 (1995) 1023–1028.
- [20] A.J. Beaudoin, H. Mecking, U.F. Kocks, *Philos. Mag.* A73 (1996) 1503–1517.
- [21] D. Raabe, M. Sachtleber, Z. Zhao, F. Roters, S. Zaefferer, *Acta Mater.* 49 (2001) 3433–3441.
- [22] D. Raabe, Z. Zhao, W. Mao, *Acta Mater.* 50 (2002) 4379–4394.
- [23] D. Raabe, Z. Zhao, S.-J. Park, F. Roters, *Acta Mater.* 50 (2002) 421–440.
- [24] D. Raabe, F. Roters, *Int. J. Plast.* 20 (2004) 339–361.
- [25] W.C. Liu, X.Y. Kong, M.B. Chen, J. Li, H. Yuan, Q.X. Yang, *Mater. Sci. Eng. A* 516 (2009) 263–269.
- [26] H.J. Bunge, *Texture Analysis in Materials Science*, Butterworths, London, 1982.
- [27] W.C. Liu, J.G. Morris, *Mater. Sci. Eng. A* 339 (2003) 183–193.
- [28] W.C. Liu, J.G. Morris, *Metall. Trans. A* 35A (2004) 265–277.
- [29] B. Bacroix, O. Brun, Th. Chauveau, *Textures Microstruct.* 14–18 (1991) 787–792.
- [30] S. Panchanadeeswaran, D.P. Field, *Acta Metall. Mater.* 43 (1995) 1683–1692.
- [31] W.C. Liu, J.G. Morris, *Scripta Mater.* 52 (2005) 1317–1321.
- [32] H.E. Vatne, R. Shahani, E. Nes, *Acta Mater.* 44 (1996) 4447–4462.
- [33] A. Duckham, R.D. Knutsen, O. Engler, *Acta Mater.* 49 (2001) 2739–2749.